Clusters in liquid fatty acids: structure and role in nucleation

Noël, John A.; Leblanc, Luc M.; Patterson, Daphne Sunita; Kreplak, Laurent; Fleischauer, Michael D.; Johnson, Erin R.; White, Mary Anne

Publisher's version / Version de l'éditeur:
https://doi.org/10.1021/acs.jpcb.9b05017
The Journal of Physical Chemistry B, 123, 32, pp. 7043-7054, 2019-07-19

THE JOURNAL OF PHYSICAL CHEMISTRY B

Article

Cite This: J. Phys. Chem. B 2019, 123, 7043−7054

pubs.acs.org/JPCB

Clusters in Liquid Fatty Acids: Structure and Role in Nucleation

John A. Noël,[†] Luc M. LeBlanc,[†] Daphne Sunita Patterson,[∥] Laurent Kreplak,[‡,§] Michael D. Fleischauer,[∥,⊥] Erin R. Johnson,[†] and Mary Anne White*[,†,‡,§]

[†]Department of Chemistry, [‡]Department of Physics and Atmospheric Science, and [§]Clean Technology Research Institute, Dalhousie University, Halifax, Nova Scotia B3H 4R2, Canada

[∥]National Research Council—Nanotechnology Research Centre, Edmonton, Alberta T6G 2M9, Canada

[⊥]Department of Physics, University of Alberta, Edmonton, Alberta T6G 2E1, Canada

Supporting Information

ABSTRACT: Saturated fatty acids are used in many consumer products and have considerable promise as phase change materials for thermal energy storage, in part because they crystallize with minimal supercooling. The latter property correlates with the existence of molecular clusters in the liquid; when heated above a threshold temperature, clusters do not immediately re-form on cooling, and supercooling results. Raman spectroscopy, density functional theory calculations, and small-angle X-ray scattering were used to reveal the size, structure, and temperature dependence of the clusters. We found that the liquid phases of fatty acids contain some ordering at all temperatures, with the molecules showing, on average, short-range alignment along their long axes. At temperatures below the threshold temperature for increased susceptibility to supercooling, clusters of more highly ordered fatty acid dimers, several hundred molecules in size, exist in the liquid. Within these clusters, the alkyl chains of the fatty acid dimers are essentially completely inserted between the alkyl chains of their longitudinal neighbors. Above the threshold temperature, fatty acid clusters are smaller in size and number. We explored how the fatty acid clusters promote bulk crystallization and show quantitatively that their presence reduces the energy barrier to crystal growth, likely by a particle-attachment-type mechanism.

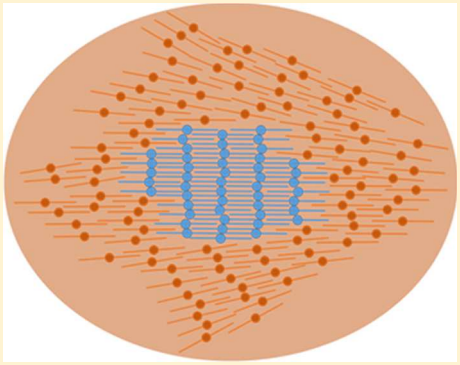

1. INTRODUCTION

Fatty acids are widespread in a variety of industrial applications, including lubricants, surfactants, foodstuff, and energy storage, but they still hold some surprises. Motivated by earlier investigations of their liquid phase,[1−4] recently, we have established that saturated fatty acids exist in clusters in the liquid state.[5] We also showed that these clusters decrease in number and/or size on heating past a threshold temperature, and the cluster reduction correlates with the onset of subsequent supercooling of fatty acids which otherwise nucleate efficiently.

Saturated fatty acids are important as phase change materials (PCMs) for thermal energy storage[6] with applications in solar thermal applications,[7] in thermal load management for electronics,[8,9] and in temperature moderation for buildings.[10−13] Therefore, knowledge of the nature and structure of the clusters in liquid fatty acids could provide insight concerning their nucleation and crystallization, both important considerations for thermal energy storage and recovery.

Although saturated fatty acids generally nucleate with little supercooling, some other promising potential PCMs, such as sugar alcohols, supercool extensively (>80 K for erythritol[14]), limiting the recovery of stored energy. In some cases, nucleating agents or external triggers can be used to induce nucleation; however, this strategy does not work for all PCMs, and is not feasible in many cases. It is thus desirable to identify potential passive mechanisms to promote nucleation in PCMs that intrinsically exhibit extensive supercooling.

Based on our recent studies,[5] we hypothesize that the clusters present in the liquid phase of fatty acids promote the formation of crystal nuclei that facilitate bulk crystallization on cooling. If there is a connection between the clusters and the growth of critical crystal nuclei, it might be possible to induce crystallization in easily supercooled materials by templating similar ordered regions in their liquid phase. While the link between the presence of clusters in the liquid phase of fatty acids and their nucleation is established, the nature of the clusters and their role in the formation of crystal nuclei have not yet been elucidated. In the present investigation, Raman spectroscopy, density functional theory (DFT) calculations, and small-angle X-ray scattering (SAXS) were used to reveal the size, structure, and temperature dependence of the clusters. With this fuller picture, the potential role of clusters in the formation of crystal nuclei in fatty acids is proposed. The importance of clusters in the nucleation of other long-chain fatty compounds also is examined.

Received: May 27, 2019
Revised: July 17, 2019
Published: July 19, 2019

DOI: 10.1021/acs.jpcb.9b05017
J. Phys. Chem. B 2019, 123, 7043−7054

2. MATERIALS AND EXPERIMENTAL METHODS

2.1. SAXS. SAXS patterns were acquired for octanoic acid (Sigma, >99%) and decanoic acid (Sigma, ≥98.0%) in the temperature range of 20−100 °C, and for dodecanoic acid (Sigma, 98%) and dodecanol (Sigma, 98%), in the range of 20−170 °C. Measurements were made on heating and cooling in 10 K steps. Scattering patterns were acquired using a Bruker-AXS NanoSTAR SAXS instrument with an Incoatec copper microsource that produced a beam of Cu Kα radiation (1.5418 Å), and a sample-to-detector distance of 34 cm. The angular range of the detector was calibrated with silver behenate. Samples of ∼0.1 mL were measured in 2 mm OD, 1.8 mm ID borosilicate glass capillaries (Charles Supper Company, Inc.) fused shut using a butane torch and a borosilicate glass rod. Capillaries were mounted in the water-cooled heating stage supplied with the SAXS instrument. Sample temperature was measured with a Pt100 resistance thermometer mounted several millimeters below the sample capillary and confirmed using a caffeine-filled capillary (caffeine powder, Sigma, Melting Point Standard). A 30 min counting time was used for each data collection. Scattering patterns were baseline-corrected with Origin 2019 software, using a linear function with three anchor points, with the same points used for each pattern.

Preliminary SAXS patterns were acquired using the Advanced Photon Source at Argonne National Laboratory on beamline 12-ID-B. Samples of octanoic acid (Sigma, >99%) were measured in a 2 mm diameter quartz tube at 25, 40, 50, and 55 °C, with a 30 s count time for each measurement.

2.2. Computational Details. Solid-state and gas-phase quantum mechanical calculations were performed to study octanoic acid in its crystalline phase and to establish the relative stabilities of the various configurations of monomeric, dimeric, and catameric units of the acid.

For the solid-state calculations performed on the "herringbone" and "stacked" crystal structures of octanoic acid (described in Section 3.1), the Quantum ESPRESSO v5.1 software package was utilized.[15] The herringbone crystal structure was obtained from the Crystallography Open Database (COD code 7050148), whereas the stacked crystal structure was manually constructed. Periodic boundary, dispersion-corrected DFT calculations utilizing B86bPBE[16,17]-XDM[18−20] were performed under the pseudopotentials/projector augmented wave formalism.[21−23] The Becke−Johnson damping parameters a_1 and a_2 in exchange-hole dipole moment (XDM) were set to 0.6512 and 1.4633 Å, respectively. Cutoffs of 80 and 600 Ry were used for the expansions of the wavefunction and density, respectively. Crystal structures were fully optimized and subjected to variable-cell relaxations, using an energy convergence threshold of 10^{-5} Ry. A 4 × 4 × 4 Monkhorst−Pack k-point grid was used for the Brillouin zone sampling. For the monomer and dimer of octanoic acid, calculations were carried out using a large vacuum cell, and the atomic coordinates were relaxed keeping the cell parameters fixed. In this case, sampling of the Brillouin zone was performed at the Γ-point.

The relative stabilities of octanoic acid dimers and catamers (Section 3.1) were further examined through the use of gas-phase calculations at the B3LYP[24−26]/6-31+G(d) level of theory, as implemented in the Gaussian 09 software package,[27] supplementing the energy and forces with the XDM dispersion correction using the postg program[28] during geometry optimization. The XDM damping parameters were set to 0.4515 and 2.1357 Å, respectively. The located stationary points were verified to be energy minima by observing no imaginary frequencies following normal-mode vibrational analyses.

Crystallographic coordinates and cell parameters, Cartesian coordinates, and additional details for the structures examined are provided in the Supporting Information.

2.3. Differential Scanning Calorimetry (DSC). The time required for bulk crystallization to begin in octanoic acid (Sigma, >99%) from the supercooled liquid phase was determined using differential scanning calorimetry (DSC; TA Instruments DSC Q200), calibrated with the melting of indium before each set of measurements. The fatty acid was heated under a 25 mL min^{-1} flow of helium past the melting point, T_{fus}, at 2 K min^{-1} to the desired temperature above T_{fus}. The sample was then held isothermally at this temperature for 60 min before being cooled at 2 K min^{-1} to a set temperature below T_{fus}, at which it was held isothermally until crystallization occurred, as evidenced by an exotherm in the DSC thermogram. The time that the sample resided in the supercooled state at the lower holding temperature before bulk crystallization occurred defined the nucleation induction time. Sample masses were ∼5 mg, and samples were measured in crimped aluminum DSC pans. Melting-/crystallization-point uncertainties were ±1 K.

2.4. Raman Spectroscopy. Raman spectra of octanoic acid (Sigma, >99%) were acquired using a Thermo Scientific Nicolet NXR 9650 Raman spectrometer. The samples were irradiated with a 1064 nm Nd:YVO_4 laser, and the Raman scattering signal was collected with an InGaAs detector. The samples were contained within 5 mm diameter glass tubes, and variable-temperature measurements were made using a liquid-nitrogen-cooled heating cell with a resistive heater. The temperature of the sample was measured outside of the sample tube, just below the laser beam path, with a type T thermocouple mounted to the surface of the cell.

3. RESULTS AND DISCUSSION

3.1. Nature of Fatty Acid Clusters. *3.1.1. Hydrogen Bonding.* Molecular clusters exist within the liquid phase of saturated fatty acids, and these clusters can be eliminated/diminished when the fatty acid is heated above a threshold temperature.[5] It is well known that fatty acids form dimers through head-to-head interactions in both the solid and liquid phases, as well as in some solutions.[2] One consideration is whether the observed change in clustering behavior corresponds to a change in the hydrogen bonding between fatty acid molecules. For example, if the fatty acid dimers dissociated into monomers, then the nature of the clusters would be different. As an individual molecule, a fatty acid would experience fewer attractive chain−chain interactions than a dimer and likely would be more mobile as its length and mass are only half that of a dimer. Another possibility is that the fatty acid dimers could rearrange themselves into a catameric structure, producing chains of molecules, which could potentially change the clusters (Figure 1).

To investigate any temperature-induced changes in fatty acid hydrogen bonding, Raman spectra of liquid octanoic acid were acquired at various temperatures (Figure 2). As the temperature was increased past the threshold temperature for increased susceptibility to supercooling for octanoic acid (∼60 °C), a vibrational band appeared just below 3500 cm^{-1}.

DOI: 10.1021/acs.jpcb.9b05017
J. Phys. Chem. B 2019, 123, 7043−7054

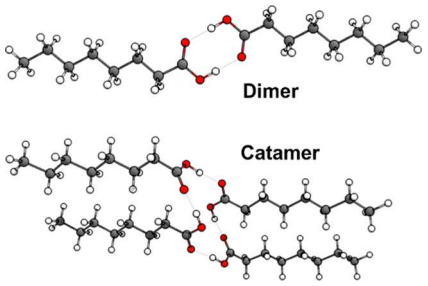

Figure 1. Comparison of fatty acid dimer and catamer structures for octanoic acid.

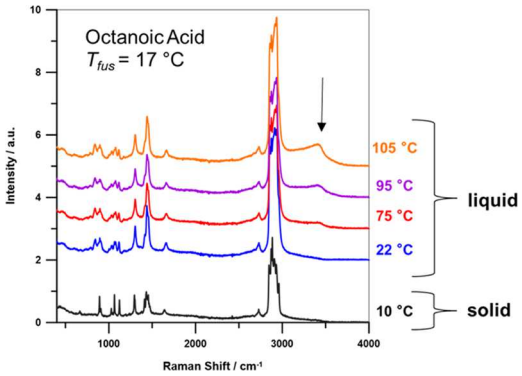

Figure 2. Raman spectra of octanoic acid in the solid phase at 10 °C and the liquid phase at various temperatures. The arrow indicates the band that appeared on heating.

This band was attributed to a stretching vibration of a free hydroxyl group.[29] When dimerized, the change in polarizability caused by the stretching of one hydroxyl group is largely offset by the corresponding change in the −OH group of the other molecule in the dimer. The result of this offset is a very weak signal in the Raman spectrum.[29] This band grew in intensity with increasing temperature, suggesting that the proportion of dissociated dimers was increasing with temperature.

However, a decrease in dimerization was not likely responsible for cluster dissociation due to the following reasons. The band attributed to free hydroxyl groups did not appear until ∼75 °C, which is above the threshold temperature for increased susceptibility to supercooling (∼60 °C). At this point, the clusters would be significantly reduced or eliminated. Second, there was no hysteresis observed in the Raman results, indicating that dissociated dimers reassociated on cooling. If a change in hydrogen bonding alone led to the loss of the clusters on heating, hysteresis would have been expected in the Raman results. Furthermore, gas-phase DFT calculations (B3LYP-XDM) showed that 37.9 kJ mol^{-1} is required to separate an octanoic acid dimer into monomeric units, whereas the thermal energy, kT, of the fatty acid at the temperatures of the Raman experiments was only ∼3 kJ mol^{-1}. As such, bulk, full dissociation of the dimers was unlikely in the melt. More likely, the appearance of the free hydroxyl stretching vibration in the Raman experiment coincides with an increase in the number of partially dissociated dimers in the liquid as the temperature is increased. Dimers likely partially dissociate and then rapidly reassociate, with the Raman spectrum giving a snapshot of the average behavior of the liquid. It is also unlikely that the fatty acids switched from dimers to catamers. Gas-phase DFT calculations (B3LYP-XDM) showed that fatty acid catamers are unstable with respect to dimers by 12.3 kJ mol^{-1}. Thus, it can be concluded that the formation and dissolution of fatty acid clusters is not related to gross changes in the hydrogen bonding of the system.

Another possible explanation for the temperature-induced changes in the clusters is related to the rotational orientation of the dimers in the bulk versus the clusters. In the high-temperature form of a solid fatty acid, the dimers adopt a "T"-shaped or herringbone orientation, as shown in Figure 3a. However, a stacked orientation, as in Figure 3b, could also be possible in the liquid phase. Solid-state DFT calculations (B86bPBE-XDM) showed the herringbone crystal structure to be favored over a crystal structure of parallel-aligned dimers by 14.4 kJ mol^{-1}. At the temperatures where clusters are observed to re-form, this energy difference is more than 4 times kT, and it is therefore unlikely that the formation and dissolution of fatty acid clusters is related to interconversion between T-shaped and stacked alignments.

3.2. Fatty Acid Cluster Structure. Our earlier NMR and dielectric constant results showed that molecular clusters in the liquid phase could be significantly reduced by heating above a fatty acid-dependent threshold temperature.[5] As described

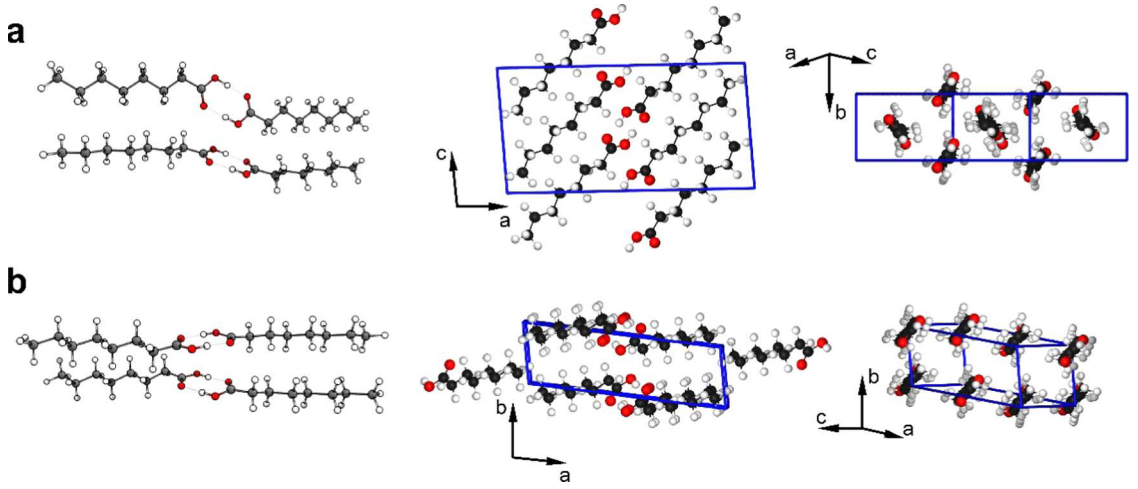

Figure 3. (a) T-shaped pairs of dimers found in the herringbone crystal structure of fatty acids (octanoic acid shown here) and (b) parallel-aligned pairs of dimers.

DOI: 10.1021/acs.jpcb.9b05017
J. Phys. Chem. B 2019, 123, 7043−7054

herein, using SAXS, the liquid-phase order of saturated fatty acids and its temperature response were investigated directly.

At high values of the scattering vector, q, two diffraction peaks have been reported previously for fatty acids.[1,30] One peak has been assigned to the lateral spacing between fatty acids and the other to the longitudinal spacing. In most of the scattering patterns acquired for the present work, only the latter was observed due to the range of scattering angles available.

SAXS patterns showing the diffraction peak corresponding to the longitudinal fatty acid spacing were acquired for octanoic, decanoic, and dodecanoic acids at 10 K increments on heating and cooling (see the Supporting Information for the full data set). At low temperature, the peaks were all asymmetrical, with excess intensity on the high-q side, and could be fit well with two Gaussians: one large peak and one smaller peak at slightly higher q (corresponding to shorter distance between scatterers), as shown in Figure 4. (One Gaussian was insufficient to give a good fit at low temperatures.)

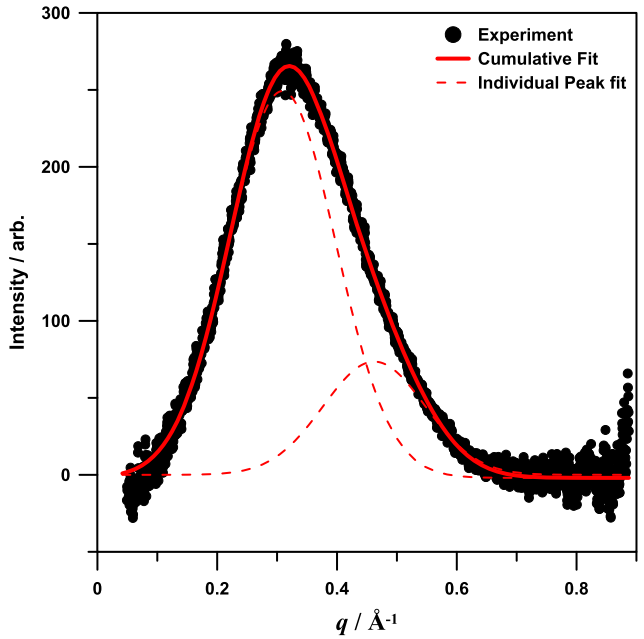

Figure 4. Fitting of the diffraction peak corresponding to the longitudinal spacing between fatty acid molecules for dodecanoic acid (T_{fus} = 43 °C) at 60 °C. The larger peak is assigned to fatty acid molecules in the bulk liquid, and the smaller peak at higher q is attributed to molecular clusters.

Upon heating, the small peak decreased in area. In dodecanoic acid (T_{fus} = 43 °C), on heating from 60 °C, the small peak continually decreased with increasing temperature, with a more dramatic decrease near dodecanoic acid's threshold temperature for increased susceptibility to supercooling (~125 °C),[5] as shown in Figures 5 and 6a. The small peak persisted to 150 °C, but at higher temperatures, the total diffraction peak was more symmetric and better fit by a single peak. In octanoic acid (Figure 6b), the small peak was present until 80 °C on heating but decreased rapidly in area starting at 60 °C, which is the approximate threshold temperature for supercooling of octanoic acid.[5] On the basis of its temperature dependence, the small peak was ascribed to fatty acid clusters. The large peak at lower q was attributed to the spacing between fatty acids in the bulk liquid. The SAXS pattern of 1-dodecanol (Supporting Information) shows only a single, symmetric peak, with similar q spacing to the peak attributed to the bulk liquid in dodecanoic acid. Clusters were not expected in 1-dodecanol, based on its supercooling behavior (Supporting Information), allowing assignment of its single diffraction peak to the bulk liquid and supporting the peak assignment for the fatty acids.

On cooling below the threshold temperature for increased susceptibility to supercooling, the asymmetry of the peaks in the fatty acids returned, signaling the return of the small peak attributed to fatty acid clusters. As the fatty acids were cooled further, the smaller peak grew in relative area, but was diminished relative to the same temperature upon heating, indicating hysteresis (Figure 6a,b). Therefore there were fewer clustered molecules on cooling than at the same temperature on heating, consistent with the DSC, NMR, and dielectric constant measurements reported previously,[5] indicating that the clusters did not re-form immediately on cooling, but that they could re-form over time.

The large peak at lower q attributed to the bulk liquid persisted well beyond the threshold temperature for supercooling of the fatty acids, at which point the fatty acid clusters were considered to be reduced or eliminated based on NMR and dielectric measurements,[5] and the higher-q small peak disappeared. Therefore, the bulk fatty acid liquid itself has some regular ordering, but it must be different from the ordering of the fatty acid clusters, based on the difference in the scattering vector at the center of each peak. Note that liquid saturated fatty acids did not exhibit any birefringence when viewed using polarized light, however. While fatty acid molecules in the bulk liquid are likely more or less aligned along their long axes, their total orientation within the liquid is likely random.

The higher value of q for the diffraction peak attributed to the fatty clusters indicates that the molecules within the clusters are more closely packed than molecules within the bulk liquid. From the values of q, the distances between scatterers were determined to be 9.8, 11.4, and 13.6 Å for clusters of octanoic acid (at 30 °C), decanoic acid (at 40 °C), and dodecanoic acid (at 60 °C), respectively, and 15.3, 17.5, and 20.4 Å for their bulk liquids, respectively (Table 1). Carboxyl headgroups of the fatty acids are the likely X-ray scattering centers as they have greater electron density than the alkyl chains. Based on the average C−C bond length for sp^3-hybridized carbon atoms in organic compounds (1.54 Å),[31] the fully extended length from the methyl carbon to the carbonyl carbon was estimated to be 13.8 Å for dodecanoic acid, 11.3 Å for decanoic acid, and 8.8 Å for octanoic acid (Table 1). However, fatty acids are known to exist primarily as dimers in the liquid phase. As such, if fatty acid dimers were stacked end to end, the observed longitudinal spacing would be expected to be the length of two fatty acid molecules.

The longitudinal spacings observed in the present work were much shorter than the length of a dimer, which implies that the fatty acid dimers are interdigitated, as previously proposed by Iwahashi et al.[30] Based on the present SAXS results, interdigitation appears to be a feature of both the clusters and the bulk liquid. The average longitudinal spacing observed for the fatty acid clusters is very close to the estimated length of a single alkyl chain (i.e., 13.8 vs 13.6 Å [observed] for dodecanoic acid; 11.3 vs 11.4 Å [observed] for decanoic acid; and 8.8 vs 9.8 Å [observed] for octanoic acid). These results

DOI: 10.1021/acs.jpcb.9b05017
J. Phys. Chem. B 2019, 123, 7043−7054

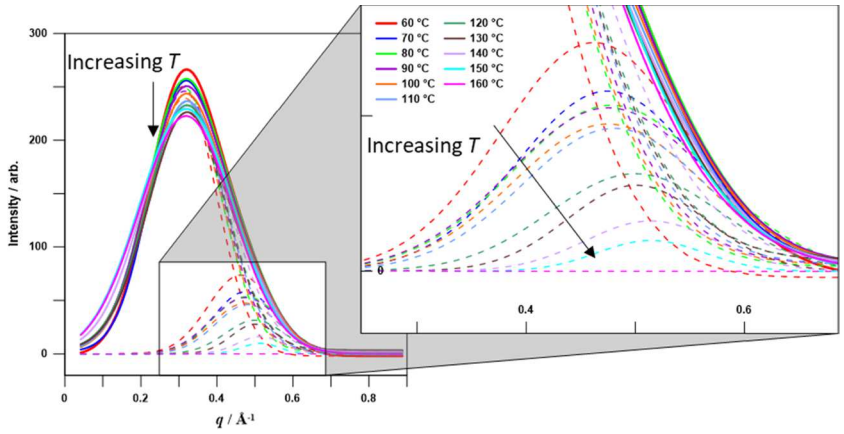

Figure 5. Cumulative peak fit (solid line) of dodecanoic acid (T_{fus} = 43 °C) at various temperatures on heating. The two peaks (dashed lines) that are summed to produce the cumulative fit (solid line) were attributed to the bulk liquid (large peak) and to fatty acid clusters (small peak). The temperature dependence of the fatty acid cluster peak is highlighted in the magnified inset.

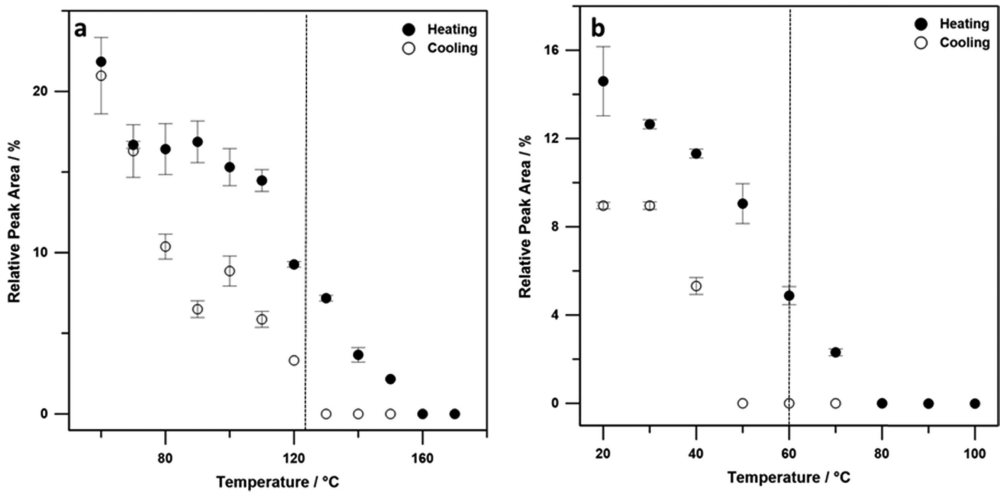

Figure 6. Relative area of the fatty acid cluster peak with respect to the peak area attributed to the bulk liquid as a function of temperature on heating and cooling for (a) dodecanoic acid (T_{fus} = 43 °C) and (b) octanoic acid (T_{fus} = 17 °C). The areas correspond to the percentage of the liquid molecules in clusters. The vertical dashed lines indicate the approximate threshold temperature for supercooling, as determined by DSC.[5] The corresponding result for decanoic acid is shown in the Supporting Information.

Table 1. Measured and Calculated Longitudinal Spacings

fatty acid	cluster (measured[a]) (Å)	bulk liquid (measured[a]) (Å)	tail-to-tail (calculated) (Å)	half-way inserted (calculated) (Å)	fully interdigitated (calculated) (Å)
octanoic acid	9.8	15.3	17.6	13.2	8.8
decanoic acid	11.4	17.5	22.6	17.0	11.3
dodecanoic acid	13.6	20.4	27.6	20.7	13.8

[a]Measured values were at 30, 40, and 60 °C for octanoic, decanoic, and dodecanoic acids, respectively.

suggest that the adjacent planes of fatty acid dimers in the clusters overlap nearly completely such that the methyl group of one fatty acid is adjacent to the carbonyl carbon of the next molecule.

Based on the q values of the peaks associated with the bulk liquid, fatty acid dimers in the bulk liquid (Figure 7a–c) are on average only about half-inserted between their longitudinal neighbors (Figure 7b). For dodecanoic acid, the observed average spacing in the bulk liquid was 20.4 Å, while the estimated spacing for half-way overlapping alkyl chains is 20.7 Å. In the bulk liquids of octanoic and decanoic acid, the observed average longitudinal spacings were 15.3 and 17.5 Å, respectively, while the estimated spacings for half-overlapped alkyl chains were 13.2 and 17.0 Å, respectively (Table 1). Based on the width of the peaks ascribed to bulk liquid, fatty acid dimers in the bulk liquid could sample any orientation from fully interdigitated to end-to-end, but on average are half-way interleaved.

On heating, the scattering peak corresponding to the bulk liquid showed little change in position (Figure 8a,b), although it did become broader. The latter suggests that the regularity of the arrangement in the liquid phase decreased and that, on heating, there was a broader distribution of longitudinal spacings between fatty acid headgroups present in the liquid.

The small peak corresponding to the fatty acid clusters both decreased in magnitude and shifted to higher q with increasing

DOI: 10.1021/acs.jpcb.9b05017
J. Phys. Chem. B 2019, 123, 7043–7054

Figure 7. Potential orderings of dimers of dodecanoic acid with (a) alkyl chains fully interdigitated, (b) half-way inserted, and (c) tail-to-tail.

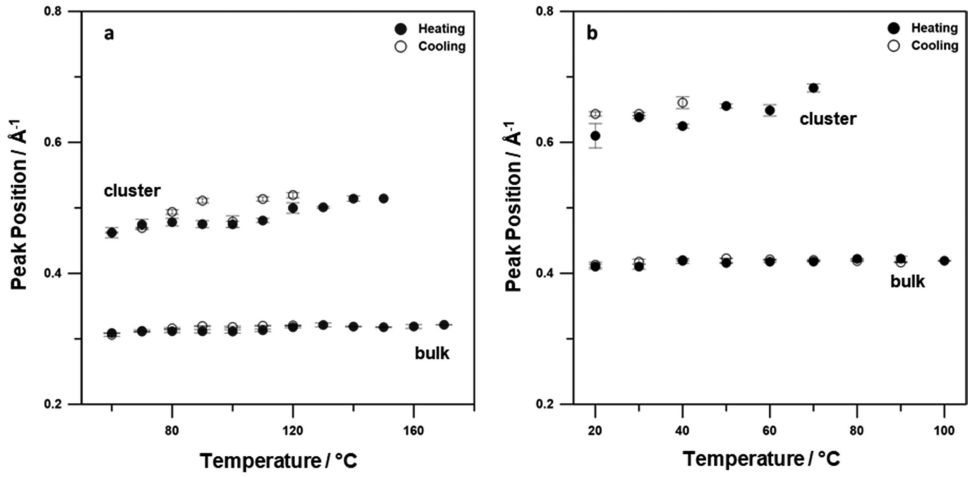

Figure 8. Peak positions of the SAXS diffraction peaks attributed to the bulk liquid and to fatty acid clusters for (a) dodecanoic acid (T_{fus} = 43 °C) and (b) octanoic acid (T_{fus} = 17 °C). The corresponding plot for decanoic acid is shown in the Supporting Information.

temperature, showing that both the number of clusters and the longitudinal spacing between fatty acids decreased on average. It could be that the more loosely packed clusters were eliminated first and the more tightly packed clusters persisted longest as the temperature increased, or this change could be associated with an increase in the lateral spacing between the fatty acid molecules. Increased lateral spacing could allow the fatty acid dimers in the clusters to become more deeply inserted between their longitudinal neighbors. For dodecanoic acid, the average longitudinal spacings in the clusters were ∼13.6 Å at 60 °C and ∼12.2 Å at 150 °C. This change in spacing corresponds to the length of ∼1.5 methylene units in an alkyl chain.

Based on the SAXS diffraction data, we now posit that the fatty acid clusters are domains of dimers that are more highly ordered and more compact than the surrounding liquid (Figure 9). The alkyl chains of the dimers in the clusters are essentially fully interdigitated whereas in the bulk liquid the dimers are roughly aligned, but less intertwined, on average. In the bulk liquid, a wider range of interheadgroup distances are found than for the clusters. Due to their full interdigitation, the clusters would be more ordered than the bulk liquid and can be thought of as smectic liquid crystalline-like domains within a nematic-like phase. In Morrow's early X-ray scattering work, he assigned the fatty acid diffraction peaks to pockets of order in an isotropic liquid;[1,32] however, it seems more likely that the entire liquid has some short-range order and that there are domains with increased order dispersed throughout the bulk.

The overall stability of the clusters could be a balance between the enthalpic stabilization of van der Waals interactions between fully interdigitated alkyl chains holding them together, and entropy, which favors their disintegration. As the temperature is increased, entropy eventually wins out and the clusters disintegrate; this crossover point could be the threshold temperature for supercooling. Above this temperature, there is not enough stabilizing energy from chain−chain interactions to overcome the entropy difference between the cluster and the bulk liquid. This reasoning agrees with previous NMR and dielectric results.[5] With regard to the intramolecular mobility (NMR), the carbon atoms within an alkyl chain fully sandwiched between its neighboring alkyl chains would have less mobility than if the alkyl chain were only partially inserted between its neighbors or if the neighboring alkyl chains were farther apart (increased lateral spacing).[5] The observed increase in slope for the curve of spin−lattice relaxation time vs temperature was likely due to the loss of the regularly ordered clusters into the less-ordered bulk liquid.[5] Similarly, the overall mobility of the fatty acids would be expected to increase if they expressed less van der Waals attraction with their neighbors. Within the clusters, a given dimer is fully surrounded by the alkyl chains of its neighbors, likely restricting its movement. However, in the bulk liquid, the movement of dimers could be less restricted and this would

DOI: 10.1021/acs.jpcb.9b05017
J. Phys. Chem. B 2019, 123, 7043−7054

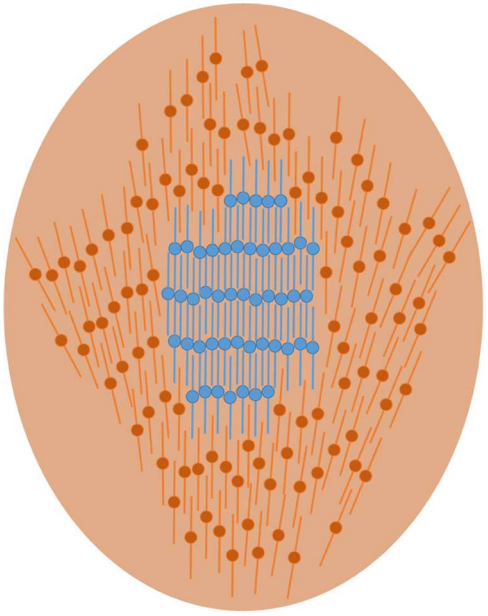

Figure 9. Schematic of the proposed ordering of fatty acid clusters (blue) in the liquid phase and of the bulk liquid (orange). The clusters are more tightly packed, and the alkyl chains of the fatty acid dimers in the cluster are nearly fully interdigitated with their longitudinal neighbors, leading to long-range order. Within a short distance, the fatty acids in the bulk liquid are roughly aligned along their long axes, but there is no restriction on how far the alkyl chains of one dimer are inserted between the alkyl chains of its longitudinal neighbors, leading to short-range order only. Fatty acid dimers in the bulk liquid are half-way interdigitated on average. Clusters are estimated to contain several hundred molecules; see the text for details. For simplicity, alkyl chains are shown as straight lines, but they would be dynamically disordered.

lead to a shift in the frequency domain $\varepsilon'(\omega)$ (dielectric constant) curve toward higher frequencies, as observed.[5]

The existence of the fatty acids as hydrogen-bonded dimers also seems important for cluster formation. Dodecanamide, which has similar hydrogen bonding to dodecanoic acid, has markedly similar supercooling behavior to dodecanoic acid (see the Supporting Information), suggesting that it too forms clusters that promote crystal growth. On the other hand, 1-dodecanol and dodecanedioic acid, which have different hydrogen-bonding motifs than dodecanoic acid, which would lead to different liquid-phase ordering, have different supercooling behaviors (see Supporting Information).

3.3. Cluster Size. The SAXS patterns acquired using synchrotron radiation (see Supporting Information Figure S12) showed a Guinier "knee" feature[33] for octanoic acid. This feature in the curve was fit using a size-distribution tool.[34] The clusters were modeled as spheroids with an 8:1 aspect ratio, as for the shape of an octanoic acid molecule. (Results did not differ significantly if the clusters were modeled as spheres.) At 25 °C, the median diameter of the fatty acid clusters in liquid octanoic acid was determined to be ~50 Å. Assuming that the molar density of the fatty acid clusters was 10% greater than the molar density of the bulk fatty acid (higher packing density in the clusters), it was estimated that the fatty acid clusters in liquid octanoic acid contained ~200 to 300 hundred molecules. As the temperature was increased, the cluster diameter decreased, dramatically dropping as the threshold temperature for increased susceptibility to supercooling in octanoic acid (~60 °C) was approached (Figure 10). This behavior correlates with the observed decrease in the fatty acid

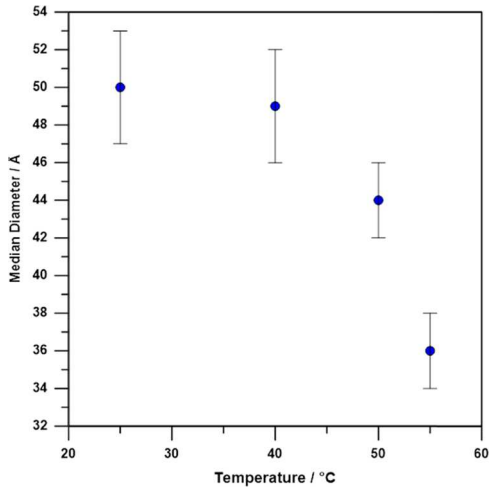

Figure 10. Median diameter of octanoic acid (T_{fus} = 17 °C) clusters as a function of temperature on heating, as determined by Guinier analysis of the SAXS pattern. The error bars represent the error in the curve fitting.

cluster diffraction peak as the clusters dissociate. At 55 °C, based on the diameter, the clusters contained fewer than 100 molecules.

3.4. Role of Fatty Acid Clusters in Nucleation. The number and size of molecular clusters in the liquid phase of linear, saturated fatty acids can be altered by heating the material above a threshold temperature. These clusters are domains of relatively well-ordered dimers with essentially full insertion of their alkyl chain between the alkyl chains of their longitudinal neighbors. With increasing temperature, the clusters break up and add to the less-ordered bulk liquid, corresponding to the onset of supercooling. Do fatty acid clusters in the liquid phase promote the formation of critical crystal nuclei?

3.4.1. Formation of a Critical Crystal Nucleus. The total Gibbs energy driving force for forming a crystal nucleus with n molecules, given by ΔG, is a balance between thermodynamic benefit of forming the stable phase (the chemical potential difference between the solid and liquid phases, $\Delta\mu$) and the formation of high-energy solid−liquid interfaces. The chemical potential difference, $\Delta\mu$, is here defined as $\mu_s - \mu_l$, where μ_s is the chemical potential of the solid phase and μ_l is the chemical potential of the liquid phase. For a crystal nucleus with only one type of surface, ΔG is[35]

$$\Delta G = n\Delta\mu + A\gamma \tag{1}$$

where A is the surface area of the crystal nucleus and γ is the interfacial energy difference between the solid and liquid phases. The chemical potential difference can be defined as:[35]

$$\Delta\mu = \frac{2\gamma V_n}{r^*} = \Delta_{fus}H\frac{T_{fus} - T}{T_{fus}} \tag{2}$$

where V_n is the volume of one molecule. Assuming a spherical shape, the critical nucleus will contain n^* molecules, with n^* defined as[35]

DOI: 10.1021/acs.jpcb.9b05017
J. Phys. Chem. B 2019, 123, 7043−7054

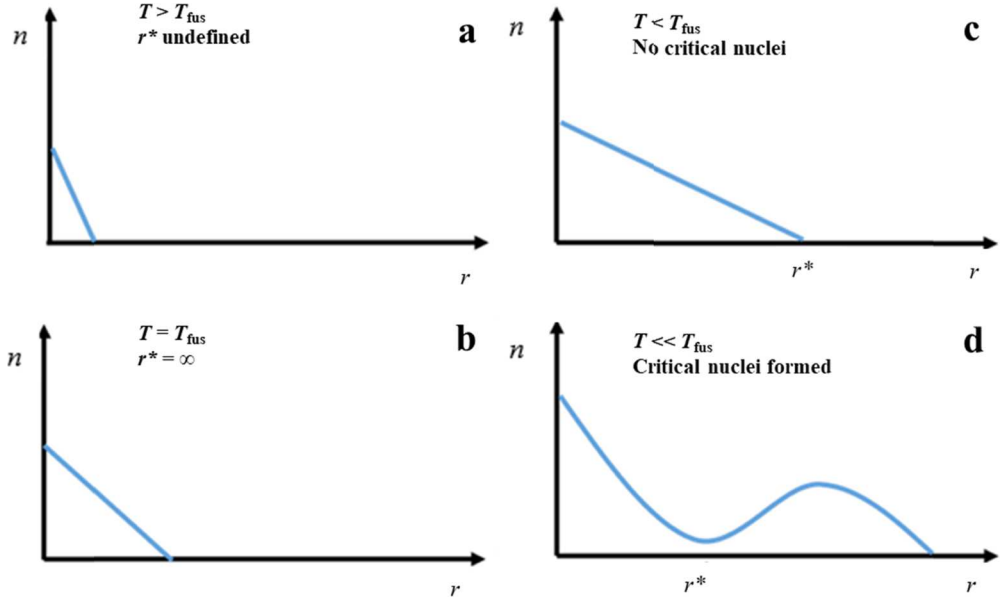

Figure 11. Schematic of the size distribution of crystal nuclei in a liquid at several temperatures, where n is the number of molecules in a cluster of radius r and r^* is the critical radius. (a) For $T > T_{fus}$, r^* is undefined and it is not possible to form a critical crystal nucleus. There are a few subcritical crystal nuclei and they are small. (b) For $T = T_{fus}$, $r^* = \infty$ and it is not possible to form a critical crystal nucleus, but there are more and larger subcritical crystal nuclei than in (a). (c) For $T < T_{fus}$, r^* has a defined value and it is possible to form critical crystal nuclei to induce bulk nucleation. As drawn, the energy barrier to form a nucleus with r^* is too high, and all crystal nuclei remain subcritical. (d) At greater supercooling, r^* becomes smaller, and crystal nuclei above the critical size are present. The critical crystal nuclei proceed to grow into larger crystals.

$$n^* = \frac{4\pi r^{*3}}{3\,V_n} \tag{3}$$

where A^* is the surface area of the spherical critical nucleus and r^* is the critical radius.

For $T \geq T_{fus}$, all crystal nuclei are thermodynamically unstable because r^* is undefined at $T > T_{fus}$ and $r^* = \infty$ at $T = T_{fus}$. Nonetheless, the liquid phase will contain some subcritical crystal nuclei in this temperature range. These crystal nuclei form dynamically as a result of density fluctuations in the liquid phase, but, due to their thermodynamic instability, quickly revert to the liquid phase. The number of nuclei and their size distribution varies with temperature (Figure 11a–d).

Substituting eqs 2 and 3 into eq 1, the energy barrier, ΔG^*, that must be overcome to form a spherical critical crystal nucleus from a supercooled liquid is

$$\Delta G^* = n^*\,\Delta\mu + A^*\gamma = \frac{16\pi V_n^{\,2}\gamma^3}{3\Delta\mu^2} + 4\pi\gamma r^{*2} \tag{4}$$

The $\frac{16\pi}{3}$ term arises from the fact that the crystal nucleus is assumed to be spherical; in a more general sense, a dimensionless shape factor, f, can be used.[35]

A cluster could form the basis of a crystal nucleus, or alternatively, crystal nuclei could grow by the agglomeration of molecular clusters. The latter processes are not taken into account by classical nucleation theory (CNuT), which hypothesizes that crystallization proceeds by attachment of monomers (atoms, molecules, or ions) to an isolated crystal nucleus. Crystal nuclei with fewer molecules than the critical number ($n < n^*$) are unstable, whereas crystal nuclei with $n > n^*$ grow to create larger crystallites. CNuT has been found to be inadequate to describe crystal nucleation in a number of systems.[36]

Recently, De Yoreo and co-workers, and others, have proposed an alternative theory, termed crystallization by particle attachment (CPA).[36−39] In the CPA theory, formation of crystal nuclei can proceed via mechanisms other than the monomer-by-monomer growth modeled by CNuT. Using CPA, a material might form prenucleation structures, such as oligomers, amorphous nanoparticles, domains of higher-density liquid, or subcritical crystalline clusters, which then coalesce to produce a bulk crystal.[36,40] Various mechanisms of CPA have been proposed for a number of mineral species and for organic macromolecules, such as proteins, and it has been suggested that many more species may undergo CPA.[41−45] Thus, it is proposed in the present work that fatty acid crystal nuclei could form using the molecular clusters (when present) as growth units. While CPA allows for this type of growth, it is not allowed by CNuT (vide infra). If crystal nucleation via the aggregation of molecular clusters were thermodynamically more favorable, or kinetically more probable, than crystal nucleation via monomer-by-monomer growth of crystal nuclei, it would account for the increased supercooling required for nucleation for fatty acids in which the clusters have been eliminated.

From eqs 2 and 4, an expression for the number of molecules required to form a critical nucleus at a given temperature, T, can be derived

$$n^* = \frac{16\pi V_n^{\,2}\gamma^3}{3\Delta_{fus}H^3\left(\frac{T_{fus}-T}{T_{fus}}\right)^3} \tag{5}$$

which shows that, at $T = T_{fus}$, an infinite number of monomers are required to form a critical nucleus, and nucleation is impossible (Figure 11b). As T decreases, the chemical potential difference increases in magnitude (eq 2), increasing the driving force for nucleation, and decreasing n^*. The dependence of critical size on temperature (from eq 5) is

DOI: 10.1021/acs.jpcb.9b05017
J. Phys. Chem. B 2019, 123, 7043−7054

plotted for dodecanoic acid in Figure 12, with n^* given in units of γ^3, which is the interfacial energy difference between the

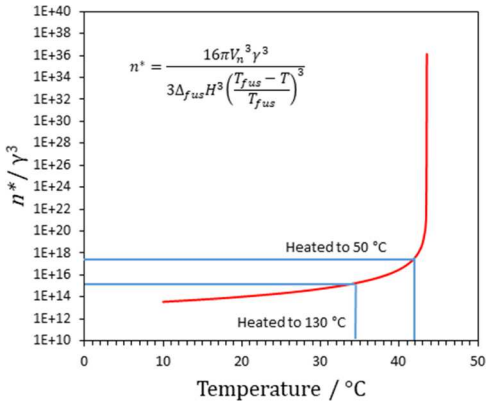

Figure 12. Number of molecules in a critical nucleus, n^*, in units of the interfacial energy difference between the solid and liquid phases, γ, as a function of temperature, T, for dodecanoic acid (T_{fus} = 43 °C) according to eq 5, based on classical nucleation theory.

solid and liquid phases. (The volume of a molecule, V_n, was estimated from the molar density of the material.) Because the value of γ for dodecanoic acid is unknown, eq 5 cannot give absolute values of n^*. However, it can illustrate differences between the numbers of molecules required to form a critical nucleus at different temperatures, provided that γ is independent of temperature.

Dodecanoic acid (T_{fus} = 43 °C) was shown previously[5] to crystallize at ca. 42 °C when heated to temperatures below its threshold temperature for increased susceptibility to supercooling (e.g., 50 °C) but crystallized at ca. 34 °C when heated above its threshold temperature for supercooling (e.g., 130 °C). From Figure 12, it can be seen that formation of critical nuclei at 42 °C would require more than 2 orders of magnitude more fatty acid molecules than at 34 °C. From a CNuT perspective, more than 100 times more individual molecular additions would be required to form a critical nucleus at 42 °C, compared to 34 °C. When nucleation occurred at 42 °C, likely molecular clusters were present in the liquid phase, and when dodecanoic acid nucleated at 34 °C, clusters were likely gone or diminished.

If fatty acid crystallization were to proceed via a CPA mechanism, and if clusters were already present in the liquid phase, it would take fewer additions to build a critical crystal nucleus than it would if there were no clusters and only individual molecules could be added to the crystal nucleus. However, these two mechanisms for growth need not be mutually exclusive. It is likely that both fatty acid dimers and metastable fatty acid clusters contribute to form a crystal nucleus.[46] By decreasing the number of additive steps required to create a critical nucleus, the probability of formation of a critical nucleus increases. Thus, the presence of clusters in the liquid phase could enhance nucleation by expediting the rate of formation of critical crystal nuclei at lower magnitudes of supercooling. Furthermore, Yoshimoto and Sato[47] showed that the rate of *cis*-9-octadecenoic acid single-crystal growth decreased when the acid had been heated to 80 °C (above its threshold temperature for increased susceptibility to supercooling) compared to when it was heated only to 20 °C. This result further supports the theory that fatty acid clusters play a role in the growth of crystal nuclei.

3.4.2. Reduction of the Energy Barrier for Nucleation. There is a thermodynamic benefit to nucleation from fatty acid clusters, as opposed to dimer-by-dimer nucleation growth, as the clusters would be enthalpically stabilized as a result of their increased density relative to the bulk liquid. The time required for crystallization to be initiated, τ_c, is related to the energy barrier for forming a critical crystal nucleus, ΔG^* (eq 6), by the Fisher–Turnbull equation[48,49]

$$\tau_c^{-1} = \frac{N_A kT}{h} e^{(-\Delta G^*/kT)} e^{(-\Delta_{dif}G/kT)} \quad (6)$$

where N_A is Avogadro's number and $\Delta_{dif}G$ is the Gibbs energy of molecular diffusion, given by[48]

$$\Delta_{dif}G = \beta T \Delta_{fus}S \quad (7)$$

where β is the fraction of molecules in the proper configuration for incorporation into a crystal nucleus and $\Delta_{fus}S$ is the entropy of fusion. Substituting eqs 2, 4, and 7 into eq 6 gives[48]

$$\tau_c^{-1} = \frac{N_A kT}{h} e^{(-16\pi V_n^2 \gamma^3 T_{fus}^2/3\Delta_{fus}H^2 kT\Delta T^2)} e^{(-\beta\Delta_{fus}S/k)} \quad (8)$$

where the degree of supercooling is $\Delta T = T_{fus} - T$. Thus[48]

$$\ln(\tau_c T) \propto \frac{1}{T\,\Delta T^2} \quad (9)$$

and a plot of $\ln(\tau_c T)$ vs $(T\,\Delta T^2)^{-1}$ yields a slope, ψ, which allows ΔG^*, the energy barrier for creating a critical crystal nucleus, to be determined from[48]

$$\Delta G^* = \frac{\psi k}{\Delta T^2} \quad (10)$$

The time required for crystallization to be initiated, τ_c, was determined at various magnitudes of supercooling for octanoic acid heated to 20 °C (below its threshold temperature for supercooling[5]) and 65 °C (above its threshold temperature for supercooling[5]). From eqs 9 and 10, values of ΔG^* at various magnitudes of supercooling were calculated for octanoic acid heated to 20 and 65 °C (Figure 13).

From Figure 13, it can be seen that the formation of a crystal nucleus was energetically more favorable when octanoic acid was heated only to 20 °C, compared to when it was heated to 65 °C, at all magnitudes of supercooling. At any given temperature below T_{fus}, the chemical potential difference between the liquid and crystalline phases was the same for both samples, regardless of thermal history, meaning that each sample had the same driving force for nucleation. However, the energetic factors working contrary to nucleation were higher for the sample heated until the molecular clusters had been eliminated or altered. Ergo, the barrier to nucleation at a given supercooling from the bulk liquid is greater than the barrier to nucleation from the molecular clusters (Figure 14). This difference could be due to clusters having lower entropy than the bulk liquid, and the entropic drop from moving from the cluster to the solid is lower in magnitude than for crystallization from the bulk liquid.

Above T_{fus}, the clusters are enthalpically stabilized by chain–chain interactions. As the liquid is heated, the clusters break apart. The temperature at which insignificant numbers of clusters are present is the threshold temperature for increased susceptibility to supercooling. At this temperature (from our previous DSC studies[5]), $kT \approx 2.7$ kJ mol^{-1} for octanoic acid and 3.3 kJ mol^{-1} for dodecanoic acid. These values likely

DOI: 10.1021/acs.jpcb.9b05017
J. Phys. Chem. B 2019, 123, 7043–7054

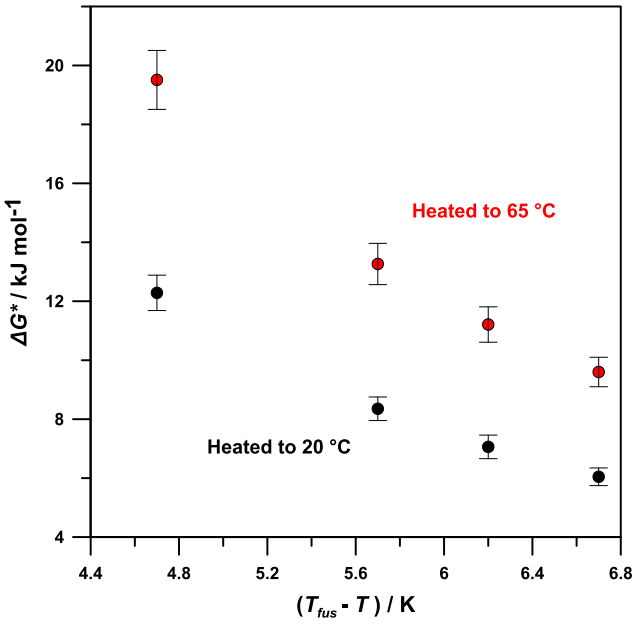

Figure 13. Gibbs energy driving force (per mole of octanoic acid) for forming a critical crystal nucleus for octanoic acid at different magnitudes of supercooling after having been heated to 20 or 65 °C (T_{fus} = 17 °C).

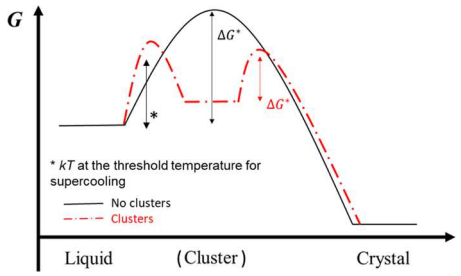

Figure 14. Schematic of the proposed energetic pathway from liquid to crystal in two models of the bulk system. Below T_{fus}, the crystalline phase is stable with respect to the liquid in both cases. In the cluster model, fatty acid clusters are proposed to be metastable with respect to the liquid. The barrier to nucleation, ΔG^*, would be lower for fatty acid clusters than for the bulk liquid. The energy barrier between the clusters and the bulk liquid is likely $\sim kT$ at the threshold temperature for supercooling.

correspond to the approximate energy barrier between the clusters and the bulk liquid.

On cooling from above the threshold temperature, there would not be a significant driving force to re-form the clusters, so clusters would not easily re-form. Without the clusters, more supercooling could be required to lower ΔG^* (by increasing the magnitude of $\Delta\mu$) to allow nucleation of the solid. The reformation of clusters could be initiated by random density fluctuations that alter the relative stabilities of the clustered and unclustered states.[3,50,51]

Ordered clusters of molecules in liquid fatty acids likely contribute to the formation of critical crystal nuclei and the growth of small crystallites. However, this growth mechanism does not imply that the clusters and the crystalline phase have the same structure. Furthermore, SAXS data indicate that the fatty acid molecules in the clusters are interdigitated, while this is not the case in the stable crystalline solid phase. Therefore, it is proposed that while the fatty acids in an initial crystal nucleus might have the same ordering as the clusters, the structure could ripen over time to the regular ordering of the crystal. Similar growth mechanisms have been observed for many other systems.[36,46,52]

Fatty acid dimers having the cluster orientation within the crystal nucleus could "remelt" and take the appropriate conformation for the stable crystal structure. Alternatively, there could be solid-state rearrangement of the domains of the crystal nucleus in which the dimers are organized as they are in the clusters. Rearrangement of the dimers in the solid state would require longitudinal neighbors to be translated across one another until they were end-to-end. Solid-state DFT calculations (B86bPBE-XDM) showed that for the herringbone crystal structure, the end-to-end configuration is stable relative to overlapping chains by ~7−12 kJ mol^{-1}, depending on the relative displacement, δ_0, of the dimers from the stable configuration (δ_0 = 0) (Figure 15a−c). As such, there could be

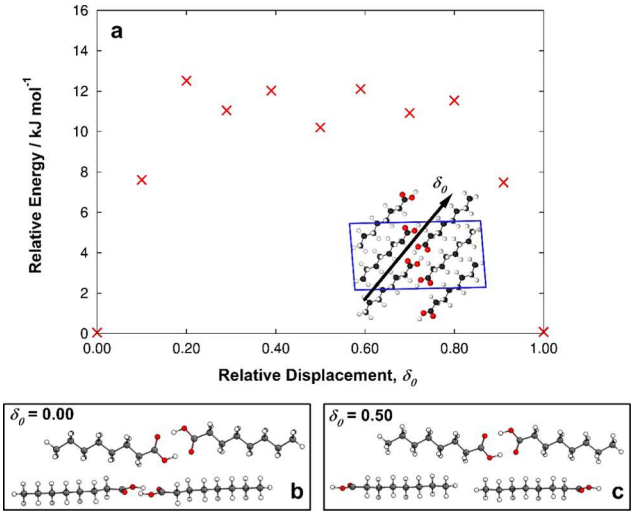

Figure 15. (a) Relative energies of different fatty acid dimer configurations with regard to the relative displacement from the stable conformation, δ_0, of adjacent dimers within a herringbone crystal structure, as calculated by solid-state DFT. (b) The initial conformation, δ_0 = 0, is the thermodynamically favored and experimentally observed conformation for adjacent dimers in a herringbone crystal structure. As one dimer is translated with respect to the other ($\delta_0 \neq 0$), the relative energy of the dimer pair increases. (c) Displacement of δ_0 = 0.5 representing the largest unique displacement.

significant energetic driving force for this rearrangement. Furthermore, once a critical nucleus has been formed and bulk crystallization commences, fatty acid dimers added to the budding crystallite could take the configuration of the stable crystalline phase.

To summarize, fatty acid clusters in the liquid phase could promote nucleation by facilitating the creation of critical crystal nuclei in fewer additive steps, relative to growth via monomers, and by reducing the nucleation energy barrier. It is proposed that, when clusters are present, critical crystal nuclei could be grown by the addition of clusters of several hundred molecules at a time, increasing the rate and probability of crystal nucleus formation. Furthermore, we have shown that the nucleation energy barrier is lower when clusters are present, and it follows that when clusters are absent, increased supercooling is needed to reduce ΔG^* and promote nucleation.

DOI: 10.1021/acs.jpcb.9b05017
J. Phys. Chem. B 2019, 123, 7043−7054

4. CONCLUSIONS

We showed that the liquid phases of fatty acids contain some ordering at all temperatures, with the molecules showing, on average, short-range alignment along their long axes. At temperatures below the threshold temperature for supercooling, clusters of more highly ordered fatty acid dimers, several hundred molecules in size, exist in the liquid. Within these clusters, the alkyl chains of the fatty acid dimers are essentially completely inserted between the alkyl chains of their longitudinal neighbors. Above a threshold temperature, fatty acid clusters are smaller and diminish in number, and the clusters are slow to re-form on cooling.

The ordered fatty acid clusters promote the formation of critical crystal nuclei and bulk crystallization of the solid phase and, in their absence, increased supercooling is needed to initiate crystallization. We proposed that the fatty acid clusters promote bulk crystallization in two ways. First, the energy barrier for nucleation is lower when fatty acid clusters were present, driven by both entropy (the difference in entropy between the clusters and the solid is likely lower than the difference in entropy between the bulk liquid and the solid) and enthalpy (the clusters are enthalpically stabilized relative to the bulk liquid) factors. Second, there could be a kinetic benefit to having clusters present. If fatty acid crystallization could proceed via a particle-attachment-type mechanism, fewer additive steps would be required to build a critical crystal nucleus if clusters of several hundred molecules could be used as building blocks, compared to individual molecules/dimers. Dodecanamide, which has the potential for similar cluster formation, displays similar supercooling, while dodecanedioic acid and 1-dodecanol, which have different aggregation structures in the liquid phase, do not. This finding supports the proposed role of clusters in promoting crystal nucleus growth.

The results presented in this study indicate that the presence of locally ordered domains within the liquid phase can assist nucleation and minimize supercooling. An example application would be a strategy to suppress supercooling in other organics with potential as PCMs: by templating domains of increased order in the liquid phase. It is posited that the creation of regions of short-range order of such molecules in the liquid phase could lower any enthalpic barrier to nucleation, while also holding the molecules in conformations more favorable for crystal nucleus formation.

■ ASSOCIATED CONTENT

Supporting Information

The Supporting Information is available free of charge on the ACS Publications website at DOI: 10.1021/acs.jpcb.9b05017.

Experimental results for supercooling behavior in 1-decanol, dodecanamide, and dodecanedioic acid; additional SAXS results; crystallographic coordinates and cell parameters for structures computed with Quantum ESPRESSO; and Cartesian coordinates and energies for structures computed with Gaussian (PDF)

■ AUTHOR INFORMATION

Corresponding Author

*E-mail: mawhite@dal.ca.

ORCID

Luc M. LeBlanc: 0000-0003-2944-2737

Erin R. Johnson: 0000-0002-5651-468X

Mary Anne White: 0000-0001-8142-0004

Notes

The authors declare no competing financial interest.

■ ACKNOWLEDGMENTS

J.A.N. acknowledges funding from Dalhousie Research in Energy, Advanced Materials and Sustainability (DREAMS), an NSERC CREATE program. J.A.N. and L.M.L. acknowledge NSERC and the Walter C. Sumner Foundation for scholarships. E.R.J., L.K., and M.A.W. acknowledge support from NSERC of Canada, and M.A.W. also acknowledges support from the Canada Foundation for Innovation and from the Clean Technologies Research Institute at Dalhousie University. E.R.J. and L.M.L. acknowledge Compute Canada (ACEnet and Westgrid) for computational resources. The authors thank M. Johnson (Dalhousie), S. Launspach (NRC-NANO), B. Lee (APS), M. Obrovac (Dalhousie), J. M. Shaw (U Alberta), and J. Zwanziger (Dalhousie) for experimental assistance and/or discussions.

■ REFERENCES

(1) Morrow, R. M. The diffraction of x-rays in liquid normal monobasic fatty acids. *Phys. Rev.* **1928**, *31*, 10−15.

(2) Iwahashi, M.; Kasahara, Y. Dynamic molecular movements and aggregation structures of lipids in a liquid state. *Curr. Opin. Colloid Interface Sci.* **2011**, *16*, 359−366.

(3) Iwahashi, M.; Yamaguchi, Y.; Kato, T.; Horiuchi, T.; Sakurai, I.; Suzuki, M. Temperature dependence of molecular conformation and liquid structure of *cis*-9-octadecenoic acid. *J. Phys. Chem. A* **1991**, *95*, 445−451.

(4) Iwahashi, M.; Kasahara, Y.; Matsuzawa, H.; Yagi, K.; Nomura, K.; Terauchi, H.; Ozaki, Y.; Suzuki, M. Self-diffusion, dynamical molecular conformation, and liquid structures of n-saturated and unsaturated fatty acids. *J. Phys. Chem. B* **2000**, *104*, 6186−6194.

(5) Noël, J. A.; Kreplak, L.; Getangama, N. N.; de Bruyn, J. R.; White, M. A. Supercooling and nucleation of fatty acids: Influence of thermal history on the behaviour of the liquid phase. *J. Phys. Chem. B* **2018**, *122*, 12386−12395.

(6) Kahwaji, S.; Johnson, M. B.; Kheirabadi, A. C.; Groulx, D.; White, M. A. Fatty acids and related phase change materials for reliable thermal energy storage at moderate temperatures. *Sol. Energy Mater. Sol. Cells* **2017**, *167*, 109−120.

(7) Joseph, A.; Kabbara, M.; Groulx, D.; Allred, P.; White, M. A. Characterization and real-time testing of phase-change materials for solar thermal energy storage. *Int. J. Energy Res.* **2016**, *40*, 61−70.

(8) Ahmed, T.; Bhouri, M.; Groulx, D.; White, M. A. Passive thermal management of tablet PCs using phase change materials: Continuous operation. *Int. J. Therm. Sci.* **2018**, *134*, 101−115.

(9) Ma, T.; Yang, H.; Zhang, Y.; Liu, L.; Wang, X. Using phase change materials in photovoltaic systems for thermal regulation and electrical efficiency improvement: a review and outlook. *Renewable Sustainable Energy Rev.* **2015**, *43*, 1273−1284.

(10) Noël, J. A.; Kahwaji, S.; Desgrosseilliers, L.; Groulx, D.; White, M. A. Phase Change Materials. In *Storing Energy*; Letcher, T., Ed.; Elsevier: Amsterdam, 2016; pp 249−272.

(11) Sharma, A.; Tyagi, V. V.; Chen, C. R.; Buddhi, D. Review on thermal energy storage with phase change materials and applications. *Renewable Sustainable Energy Rev.* **2009**, *13*, 318−345.

(12) Zalba, B.; Marin, J. M.; Cabeza, L. F.; Mehling, H. Review on thermal energy storage with phase change: materials, heat transfer analysis and applications. *Appl. Therm. Eng.* **2003**, *23*, 251−283.

(13) Arkar, C.; Medved, S. Free cooling of a building using PCM heat storage integrated into the ventilation system. *Sol. Energy* **2007**, *81*, 1078−1087.

DOI: 10.1021/acs.jpcb.9b05017
J. Phys. Chem. B 2019, 123, 7043−7054

(14) Zeng, J. L.; Zhou, L.; Zhang, Y. F.; Sun, S. L.; Chen, Y. H.; Shu, L.; Yu, L. P.; Zhu, L.; Song, L. B.; Cao, Z. Effects of some nucleating agents on the supercooling of erythritol to be applied as phase change material. *J. Therm. Anal. Calorim.* **2017**, *129*, 1291−1299.
(15) Giannozzi, P.; Andreussi, O.; Brumme, T.; Bunau, O.; Buongiorno Nardelli, M.; Calandra, M.; Car, R.; Cavazzoni, C.; Ceresoli, D.; Cococcioni, M.; et al. Advanced capabilities for materials modelling with Quantum ESPRESSO. *J. Phys.: Condens. Matter* **2017**, *29*, No. 465901.
(16) Becke, A. D. On the large-gradient behavior of the density functional exchange energy. *J. Chem. Phys.* **1986**, *85*, 7184−7187.
(17) Perdew, J. P.; Burke, K.; Ernzerhof, M. Generalized gradient approximation made simple. *Phys. Rev. Lett.* **1996**, *77*, 3865−3868.
(18) Becke, A. D.; Johnson, E. R. Exchange-hole dipole moment and the dispersion interaction revisited. *J. Chem. Phys.* **2007**, *127*, No. 154108.
(19) Otero-de-la-Roza, A.; Johnson, E. R. Van der Waals interactions in solids using the exchange-hole dipole moment model. *J. Chem. Phys.* **2012**, *136*, No. 174109.
(20) Johnson, E. R. *Non-Covalent Interactions in Quantum Chemistry and Physics*; Otero-de-la-Roza, A., DiLabio, G., Eds.; Elsevier: Amsterdam, The Netherlands, 2017; Chapter 5, pp 169−192.
(21) Pickett, W. E. Pseudopotential methods in condensed matter applications. *Comput. Phys. Rep.* **1989**, *9*, 115−197.
(22) Payne, M. C.; Teter, M. P.; Allan, D. C.; Arias, T. A.; Joannopoulos, J. D. Iterative Minimization techniques for ab initio total-energy calculations: molecular dynamics and conjugate gradients. *Rev. Mod. Phys.* **1992**, *64*, 1045−1097.
(23) Blöchl, P. E. Projector augmented-wave method. *Phys. Rev. B* **1994**, *50*, 17953−17979.
(24) Becke, A. D. Density-functional thermochemistry. III. The role of exact exchange. *J. Chem. Phys.* **1993**, *98*, 5648−5852.
(25) Becke, A. D. Density-functional exchange-energy approximation with correct asymptotic behavior. *Phys. Rev. A* **1988**, *38*, 3098−3100.
(26) Lee, C.; Yang, W.; Parr, R. G. Development of the Colle-Salvetti correlation-energy formula into a functional of the electron density. *Phys. Rev. B* **1988**, *37*, 785−789.
(27) Frisch, M. J.; Trucks, G. W.; Schlegel, H. B.; Scuseria, G. E.; Robb, M. A.; Cheeseman, J. R.; Scalmani, G.; Barone, V.; Mennucci, B.; Petersson, G. A. et al. *Gaussian 09*, revision B.01; Gaussian, Inc.: Wallingford, CT, 2010.
(28) Otero-de-la-Roza, A.; Johnson, E. R. Non-covalent interactions and thermochemistry using XDM-corrected hybrid and range-separated hybrid density functionals. *J. Chem. Phys.* **2013**, *138*, No. 204109.
(29) Bai, K. S. Raman Spectra of some carboxylic acids. *Proc. Indian Acad. Sci.* **1940**, *11*, 212−228.
(30) Iwahashi, M.; Kasahara, Y.; Minami, H.; Matsuzawa, H.; Suzuki, M.; Ozaki, Y. Molecular behaviors of n-fatty acids in liquid state. *J. Oleo Sci.* **2002**, *51*, 157−164.
(31) *Handbook of Chemistry and Physics*, 56th ed.; Weast, R. C., Ed.; CRC Press: Cleveland, 1976.
(32) Stewart, G. W.; Morrow, R. M. Molecular space array in liquid primary normal alcohols. *Proc. Nat. Acad. Sci. U.S.A.* **1927**, *13*, 222−223.
(33) Schnablegger, H.; Singh, Y. *The SAXS Guide*, 3rd ed.; Anton Paat GmbH: Graz, Austria, 2013.
(34) Ilavsky, J.; Jemain, P. R. Irena: Tool suite for modeling and analysis of small angle scattering. *J. Appl. Crystallogr.* **2009**, *42*, 347−353.
(35) Boistelle, R. Fundamentals of Nucleation and Crystal Growth. In *Crystallization and Polymorphism of Fats and Fatty Acids*; Garti, N., Sato, K., Eds.; Marcel Dekker, Inc.: New York, 1988.
(36) De Yoreo, J. J.; Gilbert, P. U. P. A.; Sommerdijk, N. A. J. M.; Penn, R. L.; Whitelam, S.; Joester, D.; Zhang, H.; Rimer, J. D.; Navrotsky, A.; Bandfield, J. F.; et al. Crystallization by particle attachment in synthetic, biogenic, and geologic environments. *Science* **2015**, *349*, No. aaa6760.
(37) Zhang, H.; De Yoreo, J. J.; Banfield, J. F. A Unified description of attachment-based crystal growth. *ACS Nano* **2014**, *8*, 6526−6530.
(38) Gebauer, D.; Cölfen, H. Prenucleation clusters and non-classical nucleation. *Nano Today* **2011**, *6*, 564−584.
(39) Legg, B. A.; De Yoreo, J. J. The energetics of prenucleation clusters in lattice solutions. *J. Chem. Phys.* **2016**, *145*, No. 211921.
(40) Vekilov, P. G. The two-step mechanism of nucleation of crystals in solution. *Nanoscale* **2010**, *2*, 2346−2357.
(41) ten Wolde, P. R.; Frenkel, D. Enhancement of protein crystal nucleation by critical density fluctuations. *Science* **1997**, *277*, 1975−1978.
(42) Demichelis, R.; Reiteri, P.; Gale, J. D.; Quigley, D.; Gebauer, D. Stable prenucleation mineral clusters are liquid-like ionic polymers. *Nat. Commun.* **2011**, *2*, No. 590.
(43) Dey, A.; Bomans, P. H. H.; Müller, F. A.; Will, J.; Frederick, P. M.; de With, G.; Sommerdijk, N. A. J. M. The role of prenucleation clusters in surface-induced calcium phosphate crystallization. *Nat. Mater.* **2010**, *9*, 1010−1014.
(44) Gebauer, D.; Völkel, A.; Cölfen, H. Stable prenucleation calcium carbonate clusters. *Science* **2008**, *322*, 1819−1822.
(45) Kumar, M.; Luo, H.; Román-Leshkov, Y.; Rimer, J. D. SSZ-13 Crystallization by particle attachment and deterministic pathways to crystal size control. *J. Am. Chem. Soc.* **2015**, *137*, 13007−13017.
(46) Lupulescu, A. I.; Rimer, J. D. In situ imaging of silicalite-1 surface growth reveals the mechanism of crystallization. *Science* **2014**, *344*, 729−732.
(47) Yoshimoto, N.; Sato, K. Preheating effects of melt on nucleation and growth of oleic acid polymorphs. *Jpn. J. Appl. Phys.* **1994**, *33*, 2746−2749.
(48) Dasgupta, S.; Rettig, F.; Ay, P. Nucleation kinetics during melt crystallization of plant based high oleic and linoleic polyunsaturated fatty acid mixtures. *Cryst. Growth Des.* **2016**, *16*, 861−866.
(49) Ng, W. L. Nucleation behaviour of tripalmitin from a triolein solution. *J. Am. Oil Chem. Soc.* **1989**, *66*, 1103−1106.
(50) Stevenson, J. D.; Wolynes, P. G. The ultimate fate of supercooled liquids. *J. Phys. Chem. A* **2011**, *115*, 3713−3719.
(51) Yoshimoto, N.; Sato, K. Preheating effects of melt on nucleation and growth of oleic acid polymorphs. *Jpn. J. Appl. Phys.* **1994**, *33*, 2746−2749.
(52) Olson, I. C.; Blonsky, A. Z.; Tamura, N.; Kunz, M.; Pokroy, B.; Romao, C. P.; White, M. A.; Gilbert, P. U. P. A. Crystal nucleation and near-epitaxial growth in nacre. *J. Struct. Biol.* **2013**, *184*, 454−463.

DOI: 10.1021/acs.jpcb.9b05017
J. Phys. Chem. B 2019, 123, 7043−7054